Coronary flow and resistance patterns indexed by subtended myocardial mass in coronary microvascular dysfunction

Thabo Mahendiran[1,2], BMBCh, MD; Nikolaos Stalikas[1], MD; Emanuele Gallinoro[1,3], MD, PhD;
Danielle Keulards[4], MD, PhD; Koshiro Sakai[1,5,6], MD, PhD; Frederic Bouisset[1], MD; Michele Mattia Viscusi[1], MD;
Sara Corradetti[1], MD; Jeroen Sonck[1], MD, PhD; Marcel van 't Veer[4,7], MS, PhD; Adriaan Wilgenhof[1,8], MD;
Nico H.J. Pijls[4,7], MD, PhD; Carlos Collet[1], MD, PhD; Bernard De Bruyne[1,2]*, MD, PhD

*Corresponding author: Cardiovascular Center OLV, Moorselbaan 164, 9300, Aalst, Belgium.
E-mail: bernard.de.bruyne@olvz-aalst.be

This paper also includes supplementary data published online at: https://eurointervention.pcronline.com/doi/10.4244/EIJ-D-25-00229

ABSTRACT

BACKGROUND: Patients with coronary microvascular dysfunction (CMD) exhibit impaired vasodilatation of the microcirculation. This manifests as reduced microvascular resistance reserve (MRR) due to either increased resting flow (Q_{rest}; functional CMD) or decreased hyperaemic flow (Q_{hyper}; structural CMD). However, coronary flow is intimately linked to myocardial mass, potentially confounding the interpretation of flow and resistance measurements.

AIMS: We investigated the relationship between subtended myocardial mass, microvascular resistance, and coronary flow to determine whether the disturbed resistance and flow patterns seen in CMD persisted after indexing by subtended myocardial mass.

METHODS: We recruited 100 patients with angina with non-obstructive coronary arteries who underwent coronary computed tomography angiography to quantify vessel-specific subtended myocardial mass. Continuous intracoronary thermodilution was used to quantify absolute coronary flow and microvascular resistance, both at rest and during hyperaemia. Among patients with an MRR <3.0, hyperaemic microvascular resistance ($R_{\mu,hyper}$) ≥475 Wood units (WU) defined structural CMD (versus functional CMD). Flow and resistance measurements were analysed both in absolute terms and after indexing by subtended mass.

RESULTS: Mass and flow were analysed in 100 patients in the left anterior descending artery. The mean subtended myocardial mass in the structural CMD group (47.00±13.83 grams) was significantly lower than in the control group (59.64±21.69 grams; p=0.027), with no significant difference between the control group and the functional CMD group (53.75±13.99 grams; p=0.339). After indexing by the subtended mass, patients with structural CMD still had higher $R_{\mu,hyper}$ (control: 20.68±7.99 WU·kg vs structural CMD: 30.58±11.63 WU·kg; p<0.001) and lower Q_{hyper} (control: 4.56±2.20 ml/min/g vs structural CMD: 3.20±0.90 ml/min/g; p=0.013). Conversely, patients with functional CMD exhibited similar indexed values of $R_{\mu,hyper}$ and Q_{hyper} to controls.

CONCLUSIONS: Despite significantly lower subtended mass, patients with structural CMD exhibit abnormal indexed $R_{\mu,hyper}$ and Q_{hyper}, supporting the notion of hyperaemic flow restriction at the tissue level that is independent of subtended mass. However, patients with functional CMD have similar subtended myocardial mass to controls and exhibit no flow restriction during hyperaemia.

Coronary microvascular dysfunction (CMD) is defined as a decrease in the vasodilatory reserve of the coronary microcirculation. It can be diagnosed invasively using either coronary flow reserve (CFR)[1] or microvascular resistance reserve (MRR)[2], with the latter having recently been shown to be specific for the microvascular compartment[3]. A reduction in CFR or MRR can arise via one of two mechanisms. Reduced resting microvascular resistance, postulated to be related to increased nitric oxide synthase activity[4], can lead to increased resting coronary flow – a pattern referred to as functional CMD. Alternatively, an increase in minimal microvascular resistance, secondary to architectural changes to the microvasculature such as remodelling and plugging[5], can lead to a limitation of maximal hyperaemic coronary flow – a pattern defined as structural CMD.

Importantly, the classification of patients with low vasodilatory reserve into one of these CMD subtypes requires the measurement of minimal microvascular resistance, for which the exact cutoff depends on the modality being used. When using continuous thermodilution, an absolute microvascular resistance of ≥475 Wood units (WU) has been proposed[6], whilst when using bolus thermodilution, an index of microcirculatory resistance (IMR) of >25 is widely accepted[7].

However, whilst microvascular resistance and coronary flow are heavily influenced by the health of the microcirculation, they are also intimately linked to the quantity of subtended myocardial mass, which has the potential to confound the interpretation of these measurements[8]. More specifically, minimal microvascular resistance is theoretically inversely proportional to subtended myocardial mass: the larger the subtended mass, the lower the resistance, and thus, the higher the coronary flow. As a consequence, patients with smaller than average perfusion territories will naturally exhibit higher values of minimal microvascular resistance and thus risk being misdiagnosed as having structural CMD.

To address this issue, we recruited patients with angina with non-obstructive coronary arteries (ANOCA) who underwent both continuous intracoronary thermodilution – for the measurement of absolute coronary flow and microvascular resistance – and coronary computed tomography angiography (CCTA) for the quantification of vessel-specific subtended myocardial mass. We explored the relationship between subtended myocardial mass and absolute coronary flow and resistance, and we investigated whether the disturbed resistance and flow patterns seen in CMD persisted after indexing by subtended myocardial mass.

Impact on daily practice

Coronary flow is intimately linked to myocardial mass, potentially confounding the interpretation of flow and resistance measurements. In the present study, despite having significantly lower subtended mass, patients with structural coronary microvascular dysfunction (CMD) had significantly higher microvascular resistance and lower coronary flow during hyperaemia after indexing by subtended myocardial mass, supporting the notion of flow restriction at the tissue level. However, patients with functional CMD had similar subtended myocardial mass to controls and exhibited no flow restriction during hyperaemia. This study provides valuable pathophysiological insights as it confirms the flow/resistance abnormality driving symptoms in structural CMD whilst highlighting the lack of a clear pathophysiological mechanism for symptoms in functional CMD.

Methods

PATIENT POPULATION

A total of 149 patients with ANOCA were screened for study inclusion. ANOCA was defined as the absence of an angiographically significant epicardial disease, specifically no diameter stenosis >50% and no fractional flow reserve (FFR) ≤0.80. Only patients who underwent continuous intracoronary thermodilution in the left anterior descending artery (LAD) were included. Patients with a history of myocardial infarction were excluded due to the potentially confounding effect of significant myocardial scarring on the analysis.

Patients were recruited from Cardiovascular Center OLV, Aalst, Belgium, between January 2019 and May 2023. Patients were included if they (i) had previously undergone a CCTA scan permitting the calculation of subtended myocardial mass and (ii) subsequently underwent invasive coronary angiography, including an assessment for CMD using continuous intracoronary thermodilution. The median time between CCTA and the invasive assessment was 28 days (interquartile range [IQR] 9-93). All patients provided informed consent. The study protocol was approved by the institutional review board of the Onze-Lieve-Vrouw Clinic in Aalst, Belgium (registration number: 2020/033).

CCTA FOR MYOCARDIAL MASS CALCULATION

CCTA was acquired using a dual source computed tomography (CT) scanner (SOMATOM Force [Siemens Healthineers]) with 256 detectors, a pitch of 3.2, and 240 microns of spatial resolution. Before CCTA, all patients received 0.8 mg

Abbreviations

ANOCA	angina with non-obstructive coronary arteries	**CMD**	coronary microvascular dysfunction	R_μ	microvascular resistance
		FFR	fractional flow reserve	**T**	temperature of mixed blood and saline in the distal vessel
CCTA	coronary computed tomography angiography	**MRR**	microvascular resistance reserve		
		Q	absolute coronary flow	T_i	entry temperature of saline
CFR	coronary flow reserve	Q_i	saline infusion rate	**WU**	Wood units

sublingual nitroglycerine and, in addition, intravenous metoprolol if the heart rate was ≥65 beats/min. Vessel-specific myocardial mass was quantified automatically using the Voronoi algorithm with dedicated software (Synapse 3D [Fujifilm Healthcare Solutions])[9]. The Voronoi algorithm is utilised to precisely partition the left ventricular (LV) volume by associating each voxel of the LV with the nearest voxel of an adjacent coronary artery. This process effectively maps the myocardial volume subtended by each coronary artery. The algorithm works by creating a Voronoi diagram, where each region contains all points closer to a specific coronary artery voxel than to any other. This detailed partitioning enables accurate quantification of the myocardial volume supplied by each artery. The Voronoi-based segmentation algorithm has been validated in an *ex vivo* swine heart study, demonstrating excellent accuracy[9]. In addition, the approach exhibits excellent intraobserver and interobserver repeatability[10]. Subtended mass values derived from this method have also been shown to correlate closely with invasively measured myocardial perfusion[8]. In addition, the approach has since been used as a gold-standard comparator to validate new approaches to the quantification of subtended mass[11].

To convert the algorithm-derived volume into mass, the myocardial volume was multiplied by a constant representing myocardial tissue density (1.05 g/cm^3). This is a widely accepted constant in cardiovascular imaging, having been used to convert myocardial volume to mass in numerous previous studies[12-14].

STUDY PROTOCOL

CORONARY ANGIOGRAPHY
Coronary angiography was performed via radial or femoral artery access. A 6 Fr guiding catheter was used, and 0.2 mg of intracoronary isosorbide dinitrate was administered.

CONTINUOUS THERMODILUTION
A guidewire equipped with a pressure/temperature sensor (PressureWire X [Abbott]) was connected to dedicated software for trace visualisation and analysis (CoroFlow Cardiovascular System [Coroventis]) and, after zeroing, was advanced through the guiding catheter. The pressures recorded by the pressure/temperature wire and by the fluid-filled guide catheter were equalised close to the tip of the guiding catheter. The wire was advanced into the distal part of the artery, and the temperature zeroed.

For the measurement of absolute coronary flow, a dedicated monorail infusion 2.52 Fr microcatheter with four distal side holes (RayFlow [HEXACATH]) was advanced over the pressure/temperature wire and connected to the 200 ml motorised syringe of an automated injection system (Medrad Stellant [Medrad Inc., now Bayer]) filled with room temperature saline (typically between 20°C and 23°C). The infusion catheter was advanced into the artery being investigated, and its tip was positioned into the first millimetres of the vessel. Absolute resting (Q_{rest}) and hyperaemic (Q_{hyper}) flow measurements were obtained using saline infusion rates of 10 ml/min and 20 ml/min, respectively. The resting and hyperaemic infusion protocols were either performed with separate runs for resting and hyperaemic states with a manually programmed infusion pump or a single run with

an automatically programmed infusion pump[15]. Further details on performing flow measurements using coronary continuous thermodilution have been described elsewhere[16].

CORONARY FLOW AND RESISTANCE INDICES
Absolute coronary flow (Q) in ml/min was calculated as per **Equation 1**, where T_i is the temperature of the infusate at the tip of the catheter, T is the temperature of mixed saline and blood in the distal vessel, and Q_i is the saline infusion rate. Importantly, the values of T and T_i are relative to blood temperature.

$$Q = 1.08 \cdot \frac{T_i}{T} \cdot Q_i$$

Absolute resting microvascular resistance ($R_{\mu,rest}$) in WU was calculated using **Equation 2**, where $P_{a,rest}$ is central aortic pressure under resting conditions. Importantly, coronary autoregulation reduces $R_{\mu,rest}$ in the face of any epicardial resistance to ensure sufficient Q_{rest}[17]. Accordingly, the use of $P_{a,rest}$ adjusts for the presence of epicardial resistance, permitting the calculation of "true" $R_{\mu,rest}$, i.e., $R_{\mu,rest}$ as would be expected in the absence of any epicardial resistance.

$$R_{\mu,rest} = \frac{P_{a,rest}}{Q_{rest}}$$

Absolute hyperaemic microvascular resistance ($R_{\mu,hyper}$) in WU was calculated using **Equation 3**, where $P_{d,hyper}$ is the distal coronary pressure during hyperaemia:

$$R_{\mu,hyper} = \frac{P_{d,hyper}}{Q_{hyper}}$$

CFR was calculated using the following equation **(Equation 4)**:

$$CFR = \frac{Q_{hyper}}{Q_{rest}}$$

MRR was calculated with the following equation **(Equation 5)**, where $P_{a,rest}$ and $P_{a,hyper}$ correspond to aortic pressure measured during resting and hyperaemic conditions, respectively. Unlike CFR, MRR is not influenced by the presence of epicardial resistance, making it a more specific index of microvascular function[3].

$$MRR = \frac{CFR}{FFR} \cdot \frac{P_{a,rest}}{P_{a,hyper}}$$

STRATIFICATION BY CMD SUBTYPE
Given the greater specificity of MRR than CFR for the microvascular compartment[3], MRR was used to diagnose CMD, using a cutoff of <3.0, as proposed in a recent, large-scale study[18]. Patients with an MRR ≥3.0 were defined as controls. Among patients with an MRR <3.0, an $R_{\mu,hyper}$ of ≥475 WU defined structural CMD, whereas a value <475 WU defined functional CMD[6]. The cutoff of 475 WU was chosen as this represents the upper limit of the 95% confidence interval for $R_{\mu,hyper}$ in the LAD territory in normal controls[19]. This cutoff was subsequently proposed in a recent study by de Vos et al[6]. To assess the robustness of any findings, the analysis was also performed with CMD defined as a CFR <2.5[1]. For the analysis stratified by CMD subtype (control vs

functional CMD vs structural CMD), only measurements in the LAD were used, in keeping with current clinical practice[16].

INDEXING Q AND R_μ BY SUBTENDED MYOCARDIAL MASS AND BODY SURFACE AREA

The indexing of Q and R_μ values by subtended myocardial mass is based upon the following theory: the larger the subtended mass, the higher the Q and thus the lower the R_μ. Likewise, the smaller the subtended mass, the higher the R_μ and thus the lower the Q. Given that Q is proportional to mass, indexing requires Q to be divided by mass, and thus indexed Q (in ml/min/g)=Q/mass. On the other hand, as R_μ is proportional to 1/mass, indexing R_μ by mass requires R_μ to be divided by 1/mass, and thus indexed R_μ (in WU·kg)=R_μ x mass[19]. A numerical example is provided in **Supplementary Figure 1**. Indexed values were further indexed by body surface area (BSA) to adjust for the potential impact of body size on cardiac volume. BSA was calculated using the Mosteller formula[20].

STATISTICS

Continuous variables with a normal distribution are expressed as mean±standard deviation and non-normally distributed variables as median and IQR. Categorical variables are expressed as counts and percentages.

Logistic regression was used for the prediction of binary variables. Multivariate regression was used to control for potential confounding variables. The following variables were included as covariates: age, sex, body mass index, smoking, hypertension, diabetes, dyslipidaemia, previous percutaneous coronary intervention, estimated glomerular filtration rate (eGFR), LV ejection fraction, baseline medications (statin, angiotensin-converting enzyme inhibitor/angiotensin receptor blocker, aspirin, other antiplatelet, antidiabetic medication), as well as heart rate and blood pressure (both extracted at the exact time of flow measurement). The final variables included in multivariate models were selected using both forward and backward selection, with only variables with a p-value<0.05 included in the final models.

Analysis of variance (ANOVA) was used to compare the mean of a given parameter across different subgroups. If ANOVA identified a significant difference between mean values, pairwise comparisons were performed using the Bonferroni *post hoc* test to identify which specific mean values differed. To counteract the impact of multiple testing, the Bonferroni correction was applied to p-values by multiplying them by the number of comparisons performed.

As an alternative approach to control for the impact of subtended mass on $R_{\mu,hyper}$, patients with structural CMD were matched by subtended mass with control patients using propensity score matching. Balance after matching was assessed using the standardised mean difference (SMD), with an SMD <0.1 indicating an acceptable balance between groups.

All analyses were performed using Python 3.11.4 (Python Software Foundation). A p-value<0.05 was considered statistically significant.

Results

STUDY POPULATION

In total, 149 patients with ANOCA who underwent CCTA and subsequent invasive measurements of coronary flow and resistance in the LAD were screened for inclusion. Among them, 43 patients were excluded because of an FFR ≤0.80, and a further 6 patients were excluded because of a history of myocardial infarction. Thus, in total, 100 patients were included in the final analysis. The baseline clinical characteristics of the overall population are shown in **Table 1**.

ANALYSIS STRATIFIED BY CMD SUBTYPE

The population was classified into functional CMD (n=31), structural CMD (n=20), and controls (n=49). Of note, patients with structural CMD were older (control: 61.2±10.6 years, functional CMD: 61.7±10.4 years, structural CMD: 69.3±7.3 years; p=0.01), and more likely to be female (control: 36.7%, functional CMD: 58.1%, structural CMD: 75.0%; p=0.01) **(Table 1)**. The structural CMD group also had the highest prevalence of hypertension (control: 55.1%, functional CMD: 38.7%, structural CMD: 80.0%; p=0.02) and the lowest eGFR (control: 80.4±14.6 ml/min, functional CMD: 84.3±11.3 ml/min, structural CMD: 71.2±17.3 ml/min; p=0.01). However, in a multivariate logistic regression analysis, age was the only baseline characteristic independently associated with structural CMD **(Supplementary Table 1)**.

SUBTENDED MYOCARDIAL MASS

The mean subtended myocardial mass in the structural CMD group (47.00±13.83 grams) was significantly lower compared to the control group (59.64±21.69 grams; p=0.027). However, there was no significant difference in subtended mass between the control and functional CMD groups (53.75±13.99 grams; p=0.339) **(Table 2)**. In a multivariate logistic regression analysis, subtended mass was independently associated with structural CMD **(Supplementary Table 1)**.

These differences in subtended mass corresponded to differences in total LV mass, with structural CMD having lower LV mass than the control and functional CMD groups (control: 147.46±36.57 grams, functional CMD: 133.71±34.06 grams, structural CMD: 122.74±40.77 grams; p=0.032). However, the percentage of left ventricular mass subtended by the LAD was similar between groups (control: 40.22±9.57%, functional CMD: 40.70±7.36%, structural CMD: 39.56±8.71%; p=0.903).

CFR AND MRR

Compared with patients without CMD, those with functional and structural CMD had significantly lower mean CFR (control: 3.44±0.81, functional CMD: 2.00±0.45, structural CMD: 1.97±0.56; p<0.001) **(Figure 1A)** and MRR (control: 3.96±0.76, functional CMD: 2.31±0.49, structural CMD: 2.16±0.63; p<0.001) **(Figure 1B, Table 2)**. Of note, there were no significant differences in CFR and MRR between the functional and structural CMD groups **(Figure 1A, Figure 1B)**.

FLOW AND RESISTANCE IN FUNCTIONAL CMD

As per its definition, the functional CMD group had a significantly higher mean Q_{rest} (117.18±38.68 ml/min) compared to the control group (71.04±18.33 ml/min; p<0.001), but there was no significant difference in mean Q_{hyper} between these two groups (control: 241.09±72.87 ml/min, functional CMD: 222.40±46.35 ml/min; p=0.364) **(Figure 2A, Table 2)**.

Table 1. Baseline characteristics of the study population, stratified by CMD subtype.

Characteristic	Overall (n=100)	No CMD (n=49)	Functional CMD (n=31)	Structural CMD (n=20)	p-value
Age, years	63.0±10.4	61.2±10.6	61.7±10.4	69.3±7.3	0.01*
Female	51 (51.0)	18 (36.7)	18 (58.1)	15 (75.0)	0.01*
BMI, kg/m²	27.3±4.7	27.3±5.1	26.7±4.5	28.4±3.9	0.49
BSA, m²	1.9±0.2	2.0±0.2	1.9±0.2	1.8±0.2	0.13
Current smoker	16 (16.0)	8 (16.3)	7 (22.6)	1 (5.0)	0.25
Smoking history	28 (28.0)	13 (26.5)	9 (29.0)	6 (30.0)	0.95
Hypertension	55 (55.0)	27 (55.1)	12 (38.7)	16 (80.0)	0.02*
Diabetes	18 (18.0)	6 (12.2)	5 (16.1)	7 (35.0)	0.08
Dyslipidaemia	74 (74.0)	36 (73.5)	21 (67.7)	17 (85.0)	0.39
FH of CAD	10 (10.0)	6 (12.2)	4 (12.9)	0 (0.0)	0.25
Previous PCI	5 (5.0)	2 (4.1)	2 (6.5)	1 (5.0)	0.89
eGFR, ml/min/1.73 m²	79.8±14.9	80.4±14.6	84.3±11.3	71.2±17.3	0.01*
LVEF, %	58.0±8.3	57.5±8.9	58.1±7.5	59.0±8.3	0.77
Statin	61 (61.0)	28 (57.1)	17 (54.8)	16 (80.0)	0.15
ACEi/ARBs	29 (29.0)	14 (28.6)	7 (22.6)	8 (40.0)	0.41
Aspirin	30 (30.0)	16 (32.7)	5 (16.1)	9 (45.0)	0.08
Anticoagulation	8 (8.0)	5 (10.2)	0 (0.0)	3 (15.0)	0.11
Oral antidiabetic	13 (13.0)	4 (8.2)	4 (12.9)	5 (25.0)	0.17
Insulin	1 (1.0)	1 (2.0)	0 (0.0)	0 (0.0)	0.59

Data are n (%) or mean±standard deviation. *Indicates statistical significance. ACEi: angiotensin-converting enzyme inhibitors; ARB: angiotensin II receptor blockers; BMI: body mass index; BSA: body surface area; CAD: coronary artery disease; CMD: coronary microvascular dysfunction; eGFR: estimated glomerular filtration rate; FH: family history; LVEF: left ventricular ejection fraction; PCI: percutaneous coronary intervention

These findings were also reflected in the measured resistances, with a lower mean $R_{\mu,rest}$ in the functional CMD group (842.03±240.70 WU) compared to the control group (1,385.11±380.67 WU; p<0.001), and similar mean $R_{\mu,hyper}$ between these two groups (control: 355.78±93.43 WU, functional CMD: 362.84±63.51 WU; p=0.951) **(Figure 2B, Table 2)**.

Importantly, these patterns persisted after indexing by subtended mass, with high indexed Q_{rest} (control: 1.36±0.70 ml/min/g, functional CMD: 2.31±0.86 ml/min/g; p<0.001), low indexed $R_{\mu,rest}$ (control: 80.82±31.30 WU·kg, functional CMD: 45.07±17.98 WU·kg; p<0.001), but normal indexed values of Q_{hyper} (control: 4.56±2.20 ml/min/g, functional CMD: 4.39±1.32 ml/min/g; p=1.000) and $R_{\mu,hyper}$ (control: 20.68±7.99 WU·kg, functional CMD: 19.33±5.68 WU·kg; p=0.757) **(Figure 2C, Figure 2D, Table 2)**. These findings also persisted after further indexation by BSA **(Supplementary Figure 2A, Supplementary Figure 2B)**.

Of note, the functional CMD group also exhibited a significantly higher resting heart rate than controls (control: 66.06±11.85 bpm, functional CMD: 76.58±13.93 bpm; p=0.001), with resting heart rate also shown to be an independent predictor of absolute Q_{rest} and $R_{\mu,rest}$ **(Supplementary Table 2)**. Furthermore, in multivariate logistic regression, resting heart rate was an independent predictor of functional CMD (p=0.006).

FLOW AND RESISTANCE IN STRUCTURAL CMD
Structural CMD had a significantly lower mean Q_{hyper} (142.76±37.42 ml/min) compared to the control group

(241.09±72.87 ml/min; p<0.001), but with no significant difference in mean Q_{rest} between these groups (control: 71.04±18.33 ml/min vs structural CMD: 80.34±41.76 ml/min; p=0.502). This corresponded to a higher mean $R_{\mu,hyper}$ (control: 355.78±93.43 WU vs structural CMD: 652.49±158.17 WU; p<0.001), but a similar mean $R_{\mu,rest}$ (control: 1,385.11±380.67 WU vs structural CMD: 1,432.36±587.84 WU; p=0.895) **(Figure 2A, Table 2)**.

These findings persisted after indexing by subtended mass for both Q_{hyper} (control: 4.56±2.20 ml/min/g vs structural CMD: 3.20±0.90 ml/min/g; p=0.013), and $R_{\mu,hyper}$ (control: 20.68±7.99 WU·kg vs structural CMD: 30.58±11.63 WU·kg; p<0.001) **(Figure 2B, Table 2)**.

Indexed Q_{rest} was also higher in the structural CMD group (control: 1.36±0.7 ml/min/g vs structural CMD: 1.85±1.16 ml/min/g; p=0.082), with a corresponding lower indexed $R_{\mu,rest}$ (control: 80.82±31.3 WU·kg vs structural CMD: 67.31±30.83 WU·kg; p=0.132), although these differences did not reach statistical significance **(Figure 2C, Figure 2D, Table 2)**.

As seen with functional CMD, patients with structural CMD had a significantly higher resting heart rate compared with controls (control: 66.06±11.85 bpm vs structural CMD: 74.64±12.39; p=0.032). However, unlike with functional CMD, heart rate was not an independent predictor of structural CMD in multivariate analysis.

The robustness of these findings was also confirmed using a propensity score-matched analysis, matching patients with structural CMD with normal controls by subtended myocardial mass **(Supplementary Table 3)**. These findings

Table 2. Mean values and standard deviations of measured parameters and calculated metrics of flow and resistance, stratified by the presence of CMD subtypes.

Parameter	Overall (n=100)	No CMD n=49	Functional CMD (n=31)	Structural CMD (n=20)	p-value
Subtended mass, g	55.29±18.66	59.64±21.69	53.75±13.99	47.00±13.83	0.03*
Total LV mass, g	138.25±37.63	147.46±36.57	133.71±34.06	122.74±40.77	0.03*
Percentage of total LV mass	40.24±8.69	40.22±9.57	40.70±7.36	39.56±8.71	0.90
CFR	2.70±0.99	3.44±0.81	2.00±0.45	1.97±0.56	<0.001*
MRR	3.09±1.08	3.96±0.76	2.31±0.49	2.16±0.63	<0.001*
FFR	0.86±0.03	0.86±0.03	0.87±0.03	0.86±0.03	0.50
Q_{rest}, ml/min	87.20±37.03	71.04±18.33	117.18±38.68	80.34±41.76	<0.001*
Mass-indexed Q_{rest}, ml/min/g	1.75±0.94	1.36±0.70	2.31±0.86	1.85±1.16	<0.001*
Q_{hyper}, ml/min	215.63±70.02	241.09±72.87	222.40±46.35	142.76±37.42	<0.001*
Mass-indexed Q_{hyper}, ml/min/g	4.23±1.82	4.56±2.20	4.39±1.32	3.20±0.90	0.02*
$R_{\mu,rest}$, WU	1,226.20±470.57	1,385.11±380.67	842.03±240.70	1,432.36±587.84	<0.001*
Mass-indexed $R_{\mu,rest}$, WU·kg	67.04±31.63	80.82±31.30	45.07±17.98	67.31±30.83	<0.001*
$R_{\mu,hyper}$, WU	417.31±155.67	355.78±93.43	362.84±63.51	652.49±158.17	<0.001*
Mass-indexed $R_{\mu,hyper}$, WU·kg	22.24±9.20	20.68±7.99	19.33±5.68	30.58±11.63	<0.001*
HR_{rest}	71.04±13.45	66.06±11.85	76.58±13.93	74.64±12.39	0.001*
HR_{hyper}	73.42±48.84	64.07±12.75	88.62±84.52	72.78±11.67	0.09
$P_{a,rest}$	93.10±13.14	93.07±12.18	90.44±12.75	97.31±15.45	0.19
$P_{a,hyper}$	93.67±14.69	92.53±13.62	90.26±14.05	101.73±15.94	0.02*

Data are mean±standard deviation. *Indicates statistical significance. Only measurements from the LAD were included. The p-value for ANOVA is shown, with pairwise comparison p-values shown in the corresponding figure. ANOVA: analysis of variance test; BSA: body surface area; CFR: coronary flow reserve; CMD: coronary microvascular dysfunction; FFR; fractional flow reserve; HR: heart rate; hyper: hyperaemic; LAD: left anterior descending artery; LV: left ventricular; MRR: microvascular resistance reserve; rest: resting; P_a: central aortic pressure; Q: absolute coronary flow; R_μ: microvascular resistance; WU: Wood units

also persisted after further indexation by BSA **(Supplementary Figure 2A, Supplementary Figure 2B)**. In addition, stratifying measurements by CFR (using a cutoff of 2.5) instead of MRR resulted in similar findings **(Supplementary Figure 3)**.

Plots of subtended mass against flow and microvascular resistance are shown in **Supplementary Figure 4**. There was no significant correlation between subtended myocardial mass and resting indices. However, subtended mass exhibited a significant correlation with hyperaemic indices (Q_{hyper} r=0.30; p=0.003; $R_{\mu,hyper}$ r=–0.29; p=0.004).

A summary of the study design and its main findings is shown in the **Central illustration**.

Discussion

The present study provides the first analysis of coronary flow and resistance patterns in CMD, both in absolute terms and after indexing by subtended myocardial mass. The principal findings of this study can be summarised as follows:
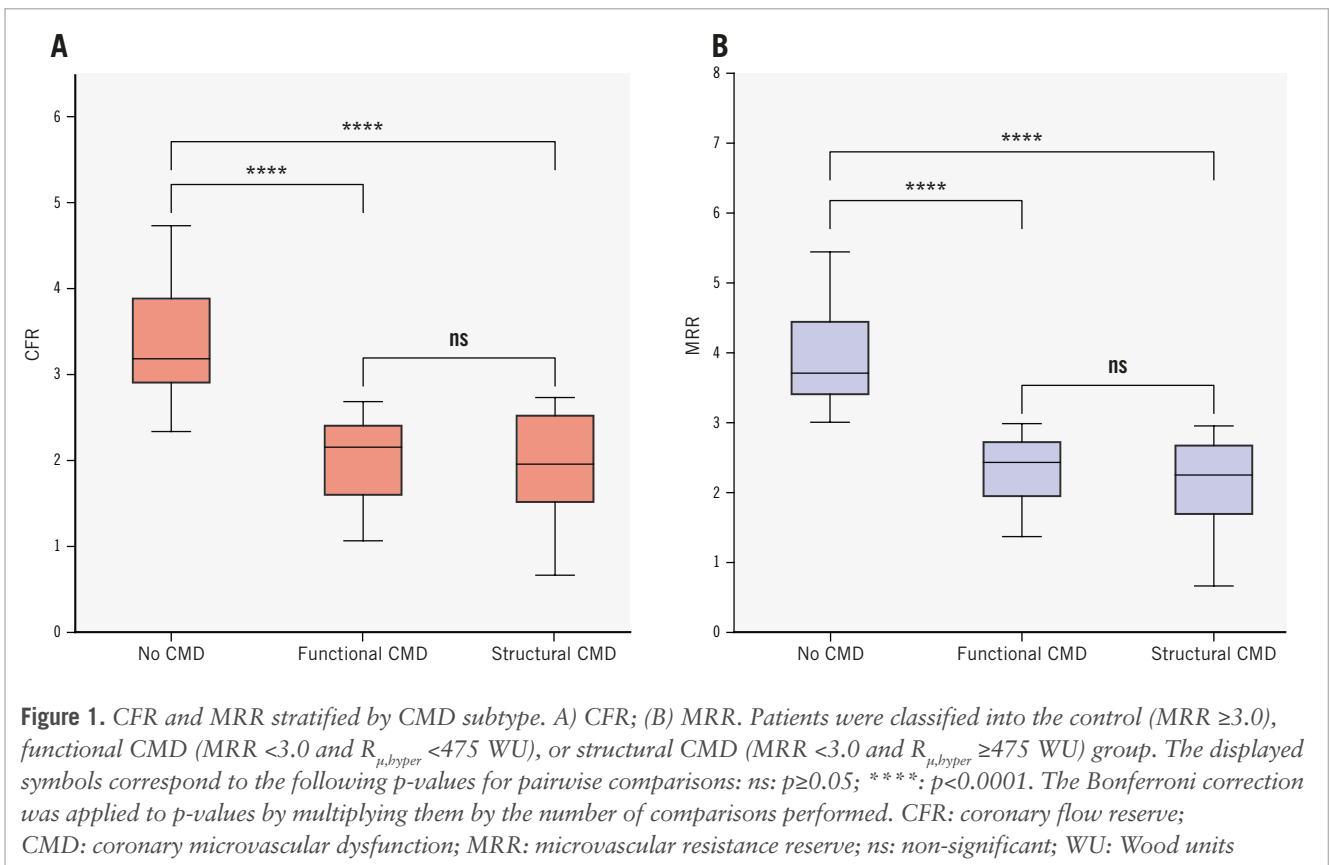i. Patients with functional CMD had similar subtended mass and exhibited similar indexed values of $R_{\mu,hyper}$ and Q_{hyper} to controls, suggesting the absence of any restriction of hyperaemic coronary flow.
ii. Patients with structural CMD, despite having significantly lower subtended myocardial mass, exhibited higher indexed $R_{\mu,hyper}$ and lower indexed Q_{hyper} than both controls and patients with functional CMD.

Taken together, these findings support the notion of restricted hyperaemic coronary flow at the tissue level in structural CMD. However, the present data also highlight the lack of a clear pathophysiological mechanism for the symptoms experienced by patients with functional CMD.

THE RELATIONSHIP BETWEEN SUBTENDED MYOCARDIAL MASS, Q AND R_μ

Whilst the relationship between subtended myocardial mass and vessel geometry (e.g., luminal diameter/area, vessel length) has long been established[21,22], data on the relationship between subtended mass and coronary flow have been limited to porcine studies and *in vitro* simulations[23]. The recent development of continuous intracoronary thermodilution has permitted the accurate and precise measurement of absolute coronary flow which, when combined with the concomitant measurement of P_a and P_d, also permits the calculation of absolute microvascular resistance[16]. Furthermore, the accuracy of the Voronoi-based segmentation algorithm for the calculation of subtended myocardial mass has already been demonstrated[9]. Keulards et al previously demonstrated the feasibility of combining continuous intracoronary thermodilution with CT-derived vessel-specific subtended myocardial mass for the calculation of myocardial perfusion[8].

It is worth noting that positron emission tomography (PET) also permits the quantification of blood flow per gram

Figure 1. *CFR and MRR stratified by CMD subtype. A) CFR; (B) MRR. Patients were classified into the control (MRR ≥3.0), functional CMD (MRR <3.0 and $R_{\mu,hyper}$ <475 WU), or structural CMD (MRR <3.0 and $R_{\mu,hyper}$ ≥475 WU) group. The displayed symbols correspond to the following p-values for pairwise comparisons: ns: p≥0.05; ****: p<0.0001. The Bonferroni correction was applied to p-values by multiplying them by the number of comparisons performed. CFR: coronary flow reserve; CMD: coronary microvascular dysfunction; MRR: microvascular resistance reserve; ns: non-significant; WU: Wood units*

of tissue (myocardial blood flow; MBF)[24]. The mean indexed Q_{rest} in the control group (1.36 ml/min/g) corresponded with the upper limit of previously reported PET MBF measured in healthy volunteers (0.7-1.2 ml/min/g)[24]. In addition, the mean indexed Q_{hyper} in the control group of 4.56 ml/min/g also corresponded with the 3- to 5-fold increase in MBF typically seen during stress with PET[25]. However, combining continuous intracoronary thermodilution and CCTA provides two distinct advantages. First, it permits the absolute quantification of total coronary blood (i.e., in ml/min) for a given artery. Second, combining invasive flow measurements with concomitant invasive pressure measurements permits the calculation of the quintessential metric of microvascular function, microvascular resistance (both total and indexed).

FUNCTIONAL CMD IS ASSOCIATED WITH NORMAL ABSOLUTE AND INDEXED $R_{\mu,HYPER}$ AND Q_{HYPER}

This study also demonstrates that the absolute flow and resistance pattern seen in functional CMD is also present after indexing by subtended myocardial mass. This finding is unsurprising given that these patients exhibited similar overall LV mass and similar quantities of myocardial mass subtended by the LAD as compared to controls. However, $R_{\mu,hyper}$ and Q_{hyper}, both in absolute terms and after indexing by subtended mass, were shown to be strictly normal in these patients, suggesting a complete absence of a disease process that limits the physiological decrease of R_μ during hyperaemia. These findings raise questions about the plausibility of the functional CMD phenotype as an explanation for exertional symptoms in these patients. Whilst increased resting nitric oxide

synthase activity is the likely explanation for the increased Q_{rest}[4], from a pathophysiological standpoint, it remains difficult to attribute patient symptoms to this finding. It is postulated that the reduced resting microvascular resistance and elevated resting coronary flow are related to increased nitric oxide synthase activity in functional CMD[4]. Yet, coronary flow is controlled by more than just nitric oxide. At any given moment, flow is carefully regulated to match current myocardial oxygen demand. A multitude of factors ultimately define myocardial oxygen demand, with heart rate, contractility, and left ventricular wall stress – i.e., mechanical factors – logically being the predominant drivers[26]. In the present study, a higher resting heart rate was seen in patients with functional CMD as compared to controls, with resting heart rate also shown to be an independent predictor of Q_{rest} and functional CMD (but not structural CMD). This finding provides a potentially interesting mechanistic insight into its pathology.

In our cohort of ANOCA patients, subtended mass exhibited a significant, weak linear relationship with flow and microvascular resistance in the hyperaemic state, with no significant relationship seen in the resting state. This suggests that other factors contribute significantly to determining coronary flow, although there are some important caveats to this finding. First, the present cohort contained many patients with CMD – both functional and structural – with the resultant impairment of resting and hyperaemic indices, respectively, likely affecting correlations. Second, during hyperaemia, the presence of concomitant epicardial disease (even non-significant) has a clear impact on Q_{hyper} which exhibits a linear
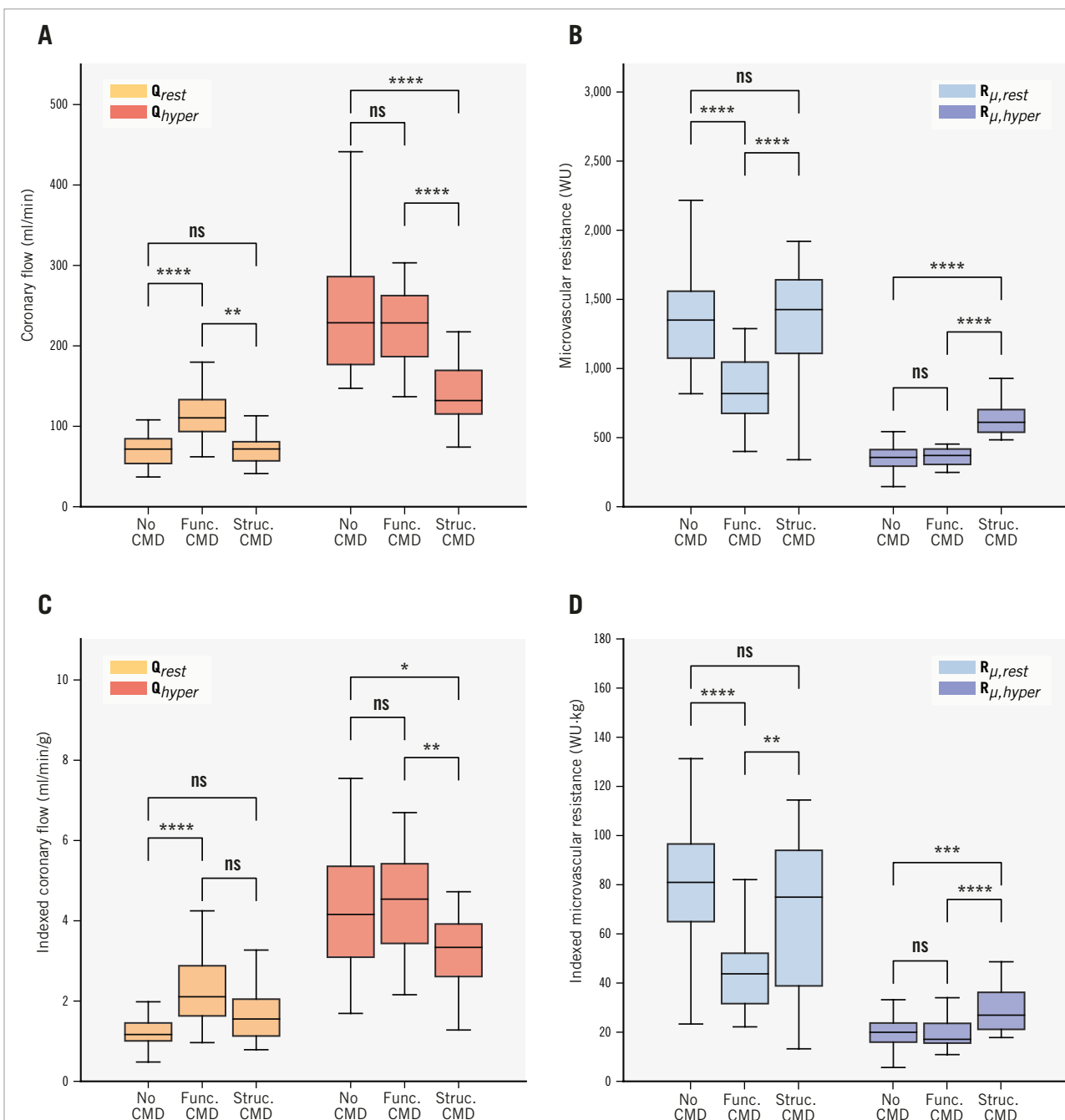
Figure 2. *Comparison of flow and microvascular resistance parameters in vessels with no CMD (MRR ≥3.0), those with functional CMD (MRR <3.0 and $R_{\mu,hyper}$ <475 WU), and those with structural CMD (MRR <3.0 and $R_{\mu,hyper}$ ≥475 WU). A) Absolute coronary flow (ml/min); (B) absolute microvascular resistance (WU); (C) indexed absolute coronary flow (ml/min/g); (D) indexed absolute microvascular resistance (WU·kg). The displayed symbols correspond to the following p-values for pairwise comparisons: ns: p≥0.05; *: p<0.05; **: p<0.01; ***: p<0.001; ****: p<0.0001. The Bonferroni correction was applied to p-values by multiplying them by the number of comparisons performed. CMD: coronary microvascular dysfunction; func.: functional; MRR: microvascular resistance reserve; ns: non-significant; Q_{hyper}: hyperaemic coronary flow; Q_{rest}: resting coronary flow; $R_{\mu,hyper}$: hyperaemic microvascular resistance; $R_{\mu,rest}$: resting microvascular resistance; struc.: structural; WU: Wood units*

relationship with FFR[17]. Given the definition of ANOCA includes patients with an FFR as low as 0.81, Q_{hyper} can be reduced to as low as 81% of what would be expected in the complete absence of epicardial disease. Importantly, in the resting state, epicardial disease has no impact on Q_{rest} unless it is extremely severe due to coronary autoregulation[17]. Third, this study likely highlights an underestimated phenomenon – the elusiveness of the "resting" state. Whilst the induction

EuroIntervention

Summary of study design and main findings.

Mass-indexed coronary flow and resistance patterns in CMD

Subtended mass confounds the interpretation of coronary flow and microvascular resistance measurements.
Do the disturbed flow and resistance patterns in CMD persist after indexing by subtended myocardial mass?
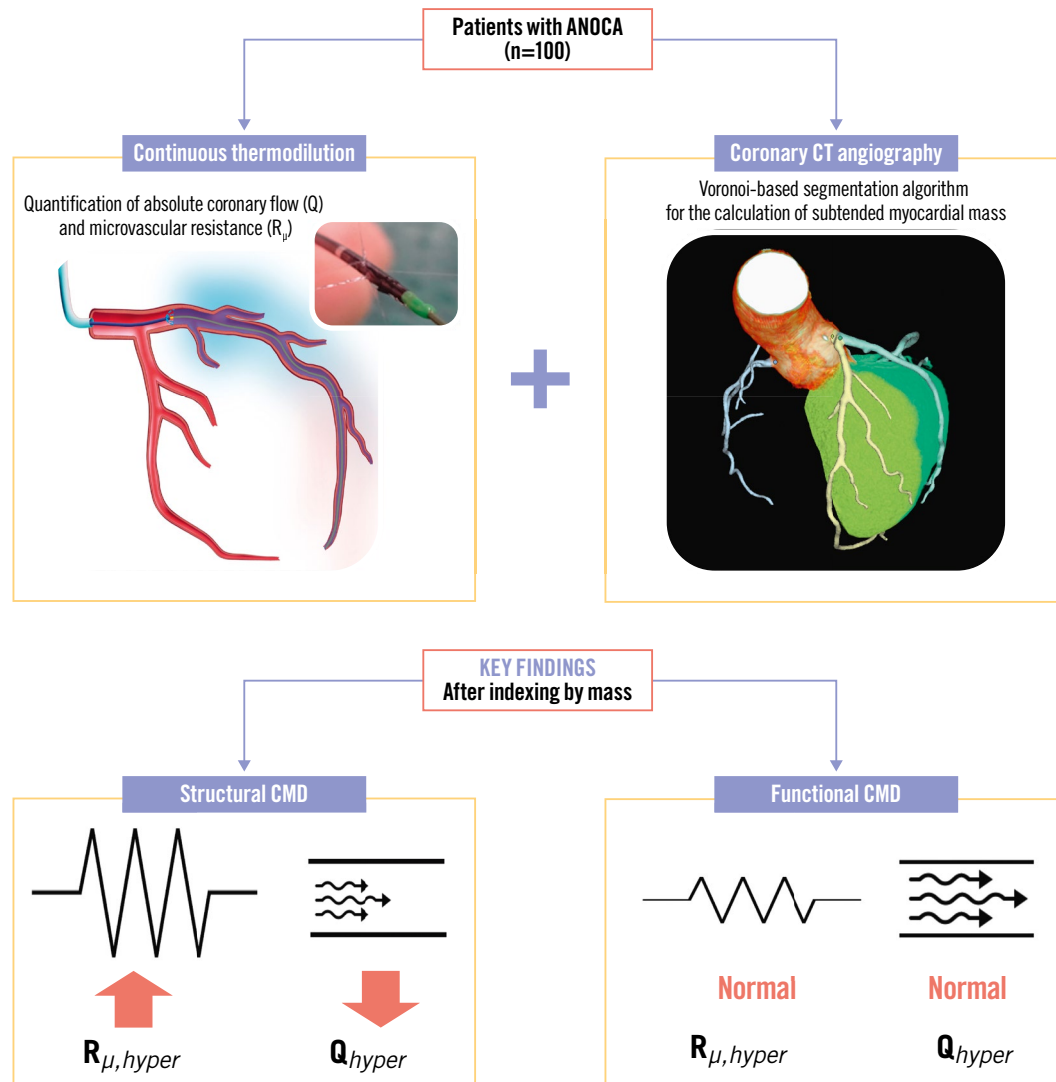
Patients with ANOCA
(n=100)

Continuous thermodilution

Quantification of absolute coronary flow (Q)
and microvascular resistance (R_μ)

Coronary CT angiography

Voronoi-based segmentation algorithm
for the calculation of subtended myocardial mass

+

KEY FINDINGS
After indexing by mass

Structural CMD

$R_{\mu,hyper}$ Q_{hyper}

Functional CMD

Normal   Normal

$R_{\mu,hyper}$ Q_{hyper}

ANOCA: angina with non-obstructive coronary arteries; CMD: coronary microvascular dysfunction; CT: computed tomography; Q_{hyper}: hyperaemic coronary flow; $R_{\mu,hyper}$: hyperaemic microvascular resistance

of maximal hyperaemia results in a consistent and repeatable decrease in $R_{\mu,hyper}$, it is not possible to assess a fixed "resting" state as microvascular resistance and coronary flow are constantly adapting to match myocardial needs, making the true "resting" state fragile and transient in nature[27]. This is further illustrated by the increased variability of flow and resistance measurements at rest as compared with hyperaemia[28]. The importance of mechanical factors that are influenced by sympathetic tone in determining resting flow raises the possibility that some patients with increased Q_{rest} may simply be manifesting increased sympathetic drive (e.g., anxiety, stress, autonomic dysfunction)[29]. We speculate that the functional CMD phenotype may, at least in part, be explained by this phenomenon.

STRUCTURAL CMD: PATTERN OF Q AND R_μ IS INDEPENDENT OF SUBTENDED MASS

Our results demonstrate that patients with structural CMD have a lower overall LV mass and a lower myocardial mass subtended by the LAD. As a consequence, the higher $R_{\mu,hyper}$ (and thus lower Q_{hyper}) seen in structural CMD could theoretically simply be attributed to the lower subtended mass seen in this group. However, our data demonstrate that these findings are independent of subtended mass, suggesting that this flow/resistance pattern persists at the gram of tissue level. This finding provides support for the notion that a pathological process at the myocardial level is responsible for the increased resistance seen in these patients[30]. Numerous architectural changes to the microvasculature have been proposed to induce structural CMD, including microcirculatory remodelling, capillary rarefaction and microcirculatory plugging[5]. It is these changes that are likely responsible for the increase in $R_{\mu,hyper}$ that manifests as a reduced vasodilatory response[4], and ultimately, the angina seen in these patients.

Limitations

First, this analysis focused on measurements in the LAD. This approach reflected current clinical practice, where it is recommended to assess CMD in this vessel[16]. However, whilst the inclusion of right coronary and left circumflex arteries would have enriched the dataset, we do not believe it would have changed the findings of this study.

Second, only continuous thermodilution was used to measure flow and resistance, as the use of other modalities such as bolus thermodilution and Doppler was not within the remit of this work. Whilst we recognise that continuous thermodilution is less widely available than bolus thermodilution, its superior precision and accuracy, along with its capacity to quantify both flow and resistance in absolute terms, justified its choice in this proof-of-concept study[31-34].

Third, only a modest number of patients were included in this study, reflecting the novel use of both CCTA and continuous intracoronary thermodilution. However, the cohort was of sufficient size to address the scientific questions addressed by this study.

Fourth, the study population includes only patients who underwent both CCTA and the invasive microvascular assessment. Whilst we frequently employ CCTA and subsequently refer patients with highly suggestive symptoms and no evidence of significant epicardial disease for an invasive evaluation, there is an inevitable risk of selection bias in this study.

Fifth, the present study stratified patients with CMD into functional/structural CMD as proposed by Rahman et al[4]. Whilst this system identifies two distinct physiological CMD subtypes, other CMD endotypes likely exist beyond this system that remain to be elucidated. Overall, it is important to recognise that the diagnosis of CMD should be made by using $R_{\mu,hyper}$ and MRR (or CFR) in conjunction, as these parameters provide complementary information on microvascular function[35].

Finally, the presence of disease processes such as diabetes, kidney disease, or hypertension could theoretically impact myocardial structure and, thus, density. However, there is currently no validated approach for adjusting the myocardial tissue density constant for the presence of such diseases. Consequently, we applied the widely accepted value of 1.05 g/cm³ for the present study[12-14].

Conclusions

Despite a significantly lower subtended mass, patients with structural CMD still exhibit abnormal indexed $R_{\mu,hyper}$ and Q_{hyper}, supporting the notion of hyperaemic flow restriction at the tissue level. However, patients with functional CMD exhibit similar indexed $R_{\mu,hyper}$ and Q_{hyper} to controls, indicating the absence of any flow restriction during hyperaemia in these patients.

Authors' affiliations

1. Cardiovascular Center Aalst, OLV Clinic, Aalst, Belgium; 2. Department of Cardiology, Lausanne University Hospital, Lausanne, Switzerland; 3. Division of University Cardiology, IRCCS Galeazzi - Sant'Ambrogio Hospital, Milan, Italy; 4. Department of Cardiology, Catharina Hospital, Eindhoven, the Netherlands; 5. Department of Medicine, Division of Cardiology, Showa University School of Medicine, Tokyo, Japan; 6. Department of Cardiology, St. Francis Hospital and Heart Center, Roslyn, NY, USA; 7. Department of Biomedical Engineering, Eindhoven University of Technology, Eindhoven, the Netherlands; 8. Department of Clinical and Molecular Medicine, Sapienza University, Rome, Italy

References

1. Ong P, Camici PG, Beltrame JF, Crea F, Shimokawa H, Sechtem U, Kaski JC, Bairey Merz CN; Coronary Vasomotion Disorders International Study Group (COVADIS). International standardization of diagnostic criteria for microvascular angina. *Int J Cardiol.* 2018;250:16-20.

2. De Bruyne B, Pijls NHJ, Gallinoro E, Candreva A, Fournier S, Keulards DCJ, Sonck J, Van't Veer M, Barbato E, Bartunek J, Vanderheyden M, Wyffels E, De Vos A, El Farissi M, Tonino PAL, Muller O, Collet C, Fearon WF.

Microvascular Resistance Reserve for Assessment of Coronary Microvascular Function: JACC Technology Corner. *J Am Coll Cardiol.* 2021;78:1541-9.

3. Mahendiran T, Bertolone D, Viscusi MM, Gallinoro E, Keulards DCJ, Collet C, Sonck J, Wilgenhof A, Pijls NHJ, De Bruyne B. The Influence of Epicardial Resistance on Microvascular Resistance Reserve. *J Am Coll Cardiol.* 2024;84:512-21.

4. Rahman H, Demir OM, Khan F, Ryan M, Ellis H, Mills MT, Chiribiri A, Webb A, Perera D. Physiological Stratification of Patients With Angina Due to Coronary Microvascular Dysfunction. *J Am Coll Cardiol.* 2020;75:2538-49.

5. Mejía-Rentería H, Lee JM, Lauri F, van der Hoeven NW, de Waard GA, Macaya F, Pérez-Vizcayno MJ, Gonzalo N, Jiménez-Quevedo P, Nombela-Franco L, Salinas P, Núñez-Gil I, Del Trigo M, Goto S, Lee HJ, Liontou C, Fernández-Ortiz A, Macaya C, van Royen N, Koo BK, Escaned J. Influence of Microcirculatory Dysfunction on Angiography-Based Functional Assessment of Coronary Stenoses. *JACC Cardiovasc Interv.* 2018;11:741-53.

6. de Vos A, Jansen TPJ, van 't Veer M, Dimitriu-Leen A, Konst RE, Elias-Smale S, Paradies V, Rodwell L, van den Oord S, Smits P, van Royen N, Pijls N, Damman P. Microvascular Resistance Reserve to Assess Microvascular Dysfunction in ANOCA Patients. *JACC Cardiovasc Interv.* 2023;16:470-81.

7. Fearon WF, Kobayashi Y. Invasive Assessment of the Coronary Microvasculature: The Index of Microcirculatory Resistance. *Circ Cardiovasc Interv.* 2017;10:e005361.

8. Keulards DCJ, Fournier S, van 't Veer M, Colaiori I, Zelis JM, El Farissi M, Zimmermann FM, Collet C, De Bruyne B, Pijls NHJ. Computed tomographic myocardial mass compared with invasive myocardial perfusion measurement. *Heart.* 2020;106:1489-94.

9. Ide S, Sumitsuji S, Yamaguchi O, Sakata Y. Cardiac computed tomography-derived myocardial mass at risk using the Voronoi-based segmentation algorithm: A histological validation study. *J Cardiovasc Comput Tomogr.* 2017;11:179-82.

10. Sumitsuji S, Ide S, Siegrist PT, Salah Y, Yokoi K, Yoshida M, Awata M, Yamasaki K, Tachibana K, Kaneda H, Nanto S, Sakata Y. Reproducibility and clinical potential of myocardial mass at risk calculated by a novel software utilizing cardiac computed tomography information. *Cardiovasc Interv Ther.* 2016;31:218-25.

11. Murai T, van de Hoef TP, van den Boogert TPW, Wijntjens GWM, Stegehuis VE, Echavarria-Pinto M, Hoshino M, Yonetsu T, Planken RN, Henriques JPS, Escaned J, Kakuta T, Piek JJ. Quantification of Myocardial Mass Subtended by a Coronary Stenosis Using Intracoronary Physiology. *Circ Cardiovasc Interv.* 2019;12:e007322.

12. Myerson SG, Montgomery HE, Whittingham M, Jubb M, World MJ, Humphries SE, Pennell DJ. Left ventricular hypertrophy with exercise and ACE gene insertion/deletion polymorphism: a randomized controlled trial with losartan. *Circulation.* 2001;103:226-30.

13. Piot C, Croisille P, Staat P, Thibault H, Rioufol G, Mewton N, Elbelghiti R, Cung TT, Bonnefoy E, Angoulvant D, Macia C, Raczka F, Sportouch C, Gahide G, Finet G, André-Fouët X, Revel D, Kirkorian G, Monassier JP, Derumeaux G, Ovize M. Effect of cyclosporine on reperfusion injury in acute myocardial infarction. *N Engl J Med.* 2008;359:473-81.

14. Shah DJ, Kim HW, James O, Parker M, Wu E, Bonow RO, Judd RM, Kim RJ. Prevalence of regional myocardial thinning and relationship with myocardial scarring in patients with coronary artery disease. *JAMA.* 2013;309:909-18.

15. Candreva A, Gallinoro E, Fernandez Peregrina E, Sonck J, Keulards DCJ, Van 't Veer M, Mizukami T, Pijls NHJ, Collet C, De Bruyne B. Automation of intracoronary continuous thermodilution for absolute coronary flow and microvascular resistance measurements. *Catheter Cardiovasc Interv.* 2022;100:199-206.

16. Belmonte M, Gallinoro E, Pijls NHJ, Bertolone DT, Keulards DCJ, Viscusi MM, Storozhenko T, Mizukami T, Mahendiran T, Seki R, Fournier S, de Vos A, Adjedj J, Barbato E, Sonck J, Damman P, Keeble T, Fawaz S, Gutiérrez-Barrios A, Paradies V, Bouisset F, Kern MJ, Fearon WF, Collet C, De Bruyne B. Measuring Absolute Coronary Flow and Microvascular Resistance by Thermodilution: JACC Review Topic of the Week. *J Am Coll Cardiol.* 2024;83:699-709.

17. Mahendiran T, Collet C, De Bruyne B. Coronary-Artery Autoregulation with Increasing Stenosis. *N Engl J Med.* 2024;390:2030-2.

18. Boerhout CKM, Lee JM, de Waard GA, Mejia-Renteria H, Lee SH, Jung JH, Hoshino M, Echavarria-Pinto M, Meuwissen M, Matsuo H, Madera-Cambero M, Eftekhari A, Effat MA, Murai T, Marques K, Doh JH, Christiansen EH, Banerjee R, Nam CW, Niccoli G, Nakayama M, Tanaka N, Shin ES, Appelman Y, Beijk MAM, van Royen N, Knaapen P, Escaned J, Kakuta T, Koo BK, Piek JJ, van de Hoef TP. Microvascular resistance reserve: diagnostic and prognostic performance in the ILIAS registry. *Eur Heart J.* 2023;44:2862-9.

19. Fournier S, Keulards DCJ, van 't Veer M, Colaiori I, Di Gioia G, Zimmermann FM, Mizukami T, Nagumo S, Kodeboina M, El Farissi M, Zelis JM, Sonck J, Collet C, Pijls NHJ, De Bruyne B. Normal values of thermodilution-derived absolute coronary blood flow and microvascular resistance in humans. *EuroIntervention.* 2021;17:e309-16.

20. Mosteller RD. Simplified calculation of body-surface area. *N Engl J Med.* 1987;317:1098.

21. Seiler C, Kirkeeide RL, Gould KL. Measurement from arteriograms of regional myocardial bed size distal to any point in the coronary vascular tree for assessing anatomic area at risk. *J Am Coll Cardiol.* 1993;21:783-97.

22. Kassab GS, Finet G. Anatomy and function relation in the coronary tree: from bifurcations to myocardial flow and mass. *EuroIntervention.* 2015;11:V13-7.

23. Choy JS, Kassab GS. Scaling of myocardial mass to flow and morphometry of coronary arteries. *J Appl Physiol (1985).* 2008;104:1281-6.

24. Schindler TH, Fearon WF, Pelletier-Galarneau M, Ambrosio G, Sechtem U, Ruddy TD, Patel KK, Bhatt DL, Bateman TM, Gewirtz H, Shirani J, Knuuti J, Gropler RJ, Chareonthaitawee P, Slart RHJA, Windecker S, Kaufmann PA, Abraham MR, Taqueti VR, Ford TJ, Camici PG, Schelbert HR, Dilsizian V. Myocardial Perfusion PET for the Detection and Reporting of Coronary Microvascular Dysfunction: A JACC: Cardiovascular Imaging Expert Panel Statement. *JACC Cardiovasc Imaging.* 2023;16:536-48.

25. Kajander SA, Joutsiniemi E, Saraste M, Pietilä M, Ukkonen H, Saraste A, Sipilä HT, Teräs M, Mäki M, Airaksinen J, Hartiala J, Knuuti J. Clinical value of absolute quantification of myocardial perfusion with (15)O-water in coronary artery disease. *Circ Cardiovasc Imaging.* 2011;4:678-84.

26. Johnson NP, Gould KL, De Bruyne B. Autoregulation of Coronary Blood Supply in Response to Demand: JACC Review Topic of the Week. *J Am Coll Cardiol.* 2021;77:2335-45.

27. Mahendiran T, Wilgenhof A, De Bruyne B. The elusiveness of "rest": the challenges of assessing resting coronary physiology. *Circulation.* 2025;152:147-9.

28. Gallinoro E, Bertolone DT, Fernandez-Peregrina E, Paolisso P, Bermpeis K, Esposito G, Gomez-Lopez A, Candreva A, Mileva N, Belmonte M, Mizukami T, Fournier S, Vanderheyden M, Wyffels E, Bartunek J, Sonck J, Barbato E, Collet C, De Bruyne B. Reproducibility of bolus versus continuous thermodilution for assessment of coronary microvascular function in patients with ANOCA. *EuroIntervention.* 2023;19:e155-66.

29. Madaric J, Bartunek J, Verhamme K, Penicka M, Van Schuerbeeck E, Nellens P, Heyndrickx GR, Wijns W, Vanderheyden M, De Bruyne B. Hyperdynamic myocardial response to beta-adrenergic stimulation in patients with chest pain and normal coronary arteries. *J Am Coll Cardiol.* 2005;46:1270-5.

30. Warisawa T, Kawase Y, Tanigaki T, Akashi YJ, Matsuo H. Structural Coronary Microvascular Dysfunction in Asymptomatic Patients With Apical Hypertrophic Cardiomyopathy. *JACC Adv.* 2023;2:100268.

31. Jansen TPJ, de Vos A, Paradies V, Dimitriu-Leen A, Crooijmans C, Elias-Smale S, Rodwell L, Maas AHEM, Smits PC, Pijls N, van Royen N, Damman P. Continuous Versus Bolus Thermodilution-Derived Coronary Flow Reserve and Microvascular Resistance Reserve and Their Association With Angina and Quality of Life in Patients With Angina and Nonobstructive Coronaries: A Head-to-Head Comparison. *J Am Heart Assoc.* 2023;12:e030480.

32. Everaars H, de Waard GA, Driessen RS, Danad I, van de Ven PM, Raijmakers PG, Lammertsma AA, van Rossum AC, Knaapen P, van Royen N. Doppler Flow Velocity and Thermodilution to Assess Coronary Flow Reserve: A Head-to-Head Comparison With [¹⁵O] H$_2$O PET. *JACC Cardiovasc Interv.* 2018;11:2044-54.

33. Gallinoro E, Bertolone DT, Mizukami T, Paolisso P, Bermpeis K, Munhoz D, Sakai K, Seki R, Ohashi H, Esposito G, Caglioni S, Mileva N, Leone A, Candreva A, Belmonte M, Storozhenko T, Viscusi MM, Vanderheyden M, Wyffels E, Bartunek J, Sonck J, Barbato E, Collet C, De Bruyne B.

Continuous vs Bolus Thermodilution to Assess Microvascular Resistance Reserve. *JACC Cardiovasc Interv.* 2023;16:2767-77.

34. Mahendiran T, Fawaz S, Viscusi M, Keulards D, Crooijmans C, Jansen TPJ, Everaars H, Gallinoro E, Candreva A, Bouisset F, Mizukami T, Bertolone D, Belmonte M, Seki R, Svanerud J, Sonck J, Wilgenhof A, Keeble TR, Damman P, Knaapen P, Collet C, Pijls NHJ, De Bruyne B. Simplification of continuous intracoronary thermodilution. *EuroIntervention.* 2024;20: e1217-26.

35. De Bruyne B, Mahendiran T. The assessment of ANOCA: coming of age? *EuroIntervention.* 2024;20:e682-3.

Supplementary data

Supplementary data

Supplementary Table 1. Multivariate logistic regression analysis of factors associated with structural CMD.

Covariate	Coefficient	p value
UNIVARIATE		
Age	0.0886	**0.003**
Female	1.2993	**0.021**
BMI	0.0586	0.282
Smoker	-1.4781	0.165
Hypertension	1.4363	**0.017**
Diabetes	1.2172	0.100
Dyslipidaemia	0.8270	0.219
eGFR	-0.0491	**0.006**
Subtended mass	-0.0385	**0.028**
MULTIVARIATE		
Age	0.0761	**0.045**
Female	0.0265	0.971
BMI	0.1074	0.165
Smoker	-0.8048	0.503
Hypertension	0.7696	0.299
Diabetes	-0.0203	0.98
Dyslipidaemia	0.3255	0.701
eGFR	-0.0426	0.075
Subtended mass	-0.0549	**0.033**
MULTIVARIATE (Age + mass only)		
Age	0.0996	**0.002**
Subtended mass	-0.0455	**0.019**

Covariates testing in multivariate analysis included: age, female sex, BMI, smoking status, hypertension, diabetes, dyslipidaemia, eGFR and subtended mass. Only age and subtended myocardial mass were independent predictors of structural CMD.

Supplementary Table 2. Univariate and multivariate linear regression analysis of the relationship between subtended myocardial mass and absolute coronary flow and resistance.
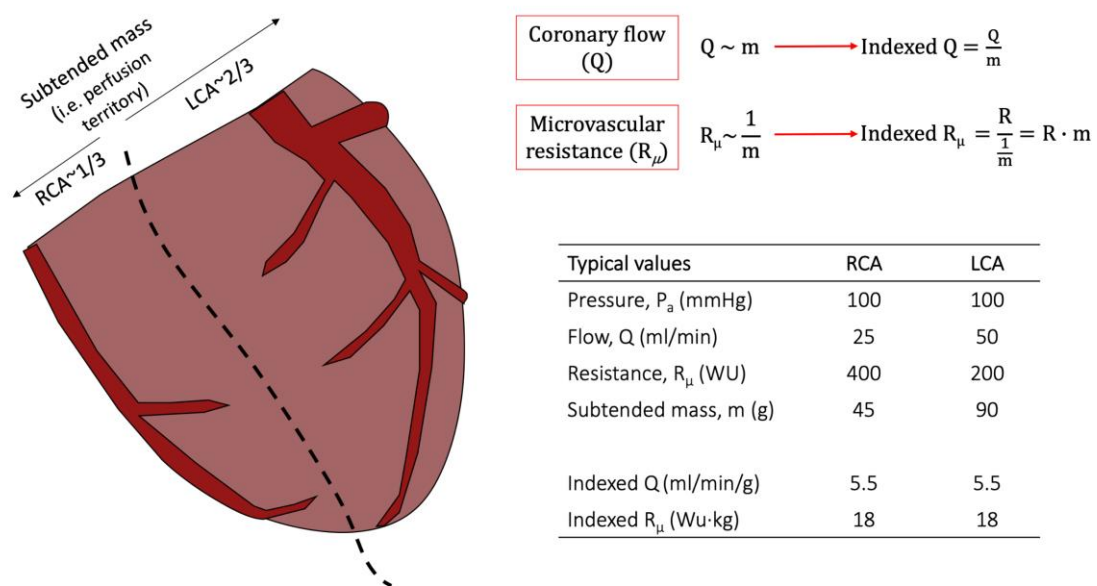
	Q_{rest}	Coefficient	p value	$R_{\mu,rest}$	Coefficient	p value	Q_{hyper}	Coefficient	p value	$R_{\mu,hyper}$	Coefficient	p value
UNIVARIATE	Subtended mass	0.041	0.839	Subtended mass	-2.192	0.390	Subtended mass	1.107	0.003	Subtended mass	-2.413	0.004
MULTIVARIATE	Resting HR	0.272	0.046	Subtended mass	-7.001	0.011	Subtended mass	1.464	<0.001	Subtended mass	-2.272	0.003
				Resting HR	-6.737	0.040	Age	-2.196	<0.001	Age	3.681	0.008
				P_a	13.867	<0.001	FFR	550.723	0.006	P_a	2.674	0.007
				Female	-220.887	0.027	P_a	1.2956	0.006			

FFR = fractional flow reserve; HR = heart rate; P_a = aortic pressure.

Supplementary Table 3. Propensity score-matched analysis.

| Parameter	Overall (n=40)	No CMD (n=20)	Structural CMD (n=20)	p value
Subtended mass (g), mean (SD)	47.00 (14.18)	47.00 (14.91)	47.00 (13.83)	0.999
Total LV mass (g), mean (SD)	125.53 (34.50)	128.46 (27.21)	122.74 (40.77)	0.608
Percentage of total LV mass, mean (SD)	38.20 (9.06)	36.76 (9.43)	39.56 (8.71)	0.342
CFR, mean (SD)	2.62 (0.89)	3.30 (0.63)	1.97 (0.56)	**<0.001**
MRR, mean (SD)	2.97 (1.04)	3.82 (0.63)	2.16 (0.63)	**<0.001**
FFR, mean (SD)	0.86 (0.03)	0.86 (0.04)	0.86 (0.03)	0.923
Q_{rest} (ml/min), mean (SD)	74.57 (32.85)	68.49 (19.01)	80.34 (41.76)	0.261
Mass-indexed Q_{rest} (ml/min/g), mean (SD)	1.74 (0.99)	1.62 (0.80)	1.85 (1.16)	0.475
Q_{hyper} (ml/min), mean (SD)	180.15 (59.65)	219.52 (53.34)	142.76 (37.42)	**<0.001**
Mass-indexed Q_{hyper} (ml/min/g), mean (SD)	4.16 (2.01)	5.16 (2.36)	3.20 (0.90)	**0.003**
$R_{\mu,rest}$ (WU), mean (SD)	1455.90 (499.03)	1480.69 (399.64)	1432.36 (587.84)	0.765
Mass-indexed $R_{\mu,rest}$ (WU·kg), mean (SD)	68.29 (28.20)	69.33 (25.96)	67.31 (30.83)	0.826
$R_{\mu,hyper}$ (WU), mean (SD)	523.44 (182.82)	387.59 (78.50)	652.49 (158.17)	**<0.001**
Mass-indexed $R_{\mu,hyper}$ (WU·kg), mean (SD)	24.51 (11.18)	18.13 (6.09)	30.58 (11.63)	**<0.001**

Given that both microvascular function and subtended mass contribute to $R_{\mu,hyper}$, patients with structural CMD were matched with controls by subtended mass. This aimed to eliminate the impact of subtended mass on flow and resistance measurements. Propensity-score matching resulted in a standardised mean difference (SMD) in subtended myocardial mass between groups of <0.01.

Subtended mass (i.e. perfusion territory)

RCA ~1/3

LCA ~2/3

Coronary flow (Q)	$Q \sim m$	→	Indexed $Q = \dfrac{Q}{m}$
Microvascular resistance (R_μ)	$R_\mu \sim \dfrac{1}{m}$	→	Indexed $R_\mu = \dfrac{R}{\frac{1}{m}} = R \cdot m$

| Typical values	RCA	LCA
Pressure, P_a (mmHg)	100	100
Flow, Q (ml/min)	25	50
Resistance, R_μ (WU)	400	200
Subtended mass, m (g)	45	90
Indexed Q (ml/min/g)	5.5	5.5
Indexed R_μ (Wu·kg)	18	18

Supplementary Figure 1. Indexing microvascular resistance and coronary flow by subtended myocardial mass.
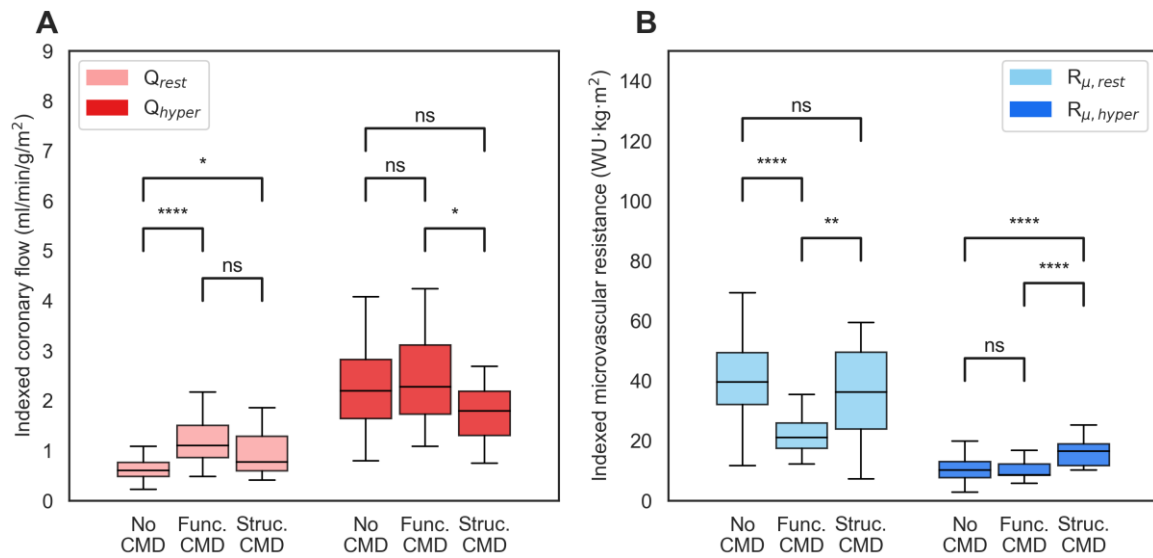
Supplementary Figure 2. Comparison of flow and microvascular resistance parameters after indexation by both subtended mass and body surface area. (**A**) Mass- and BSA-indexed coronary flow (ml/min/g/m^2), (**B**) Mass- and BSA-indexed microvascular resistance (WU·kg·m^2), The displayed symbols correspond to the following p values for pairwise comparisons: ns= ≥ 0.05, * = <0.05, ** = <0.01, *** = <0.001, **** = <0.0001. The Bonferroni correction was applied to p values by multiplying by the number of comparisons performed.
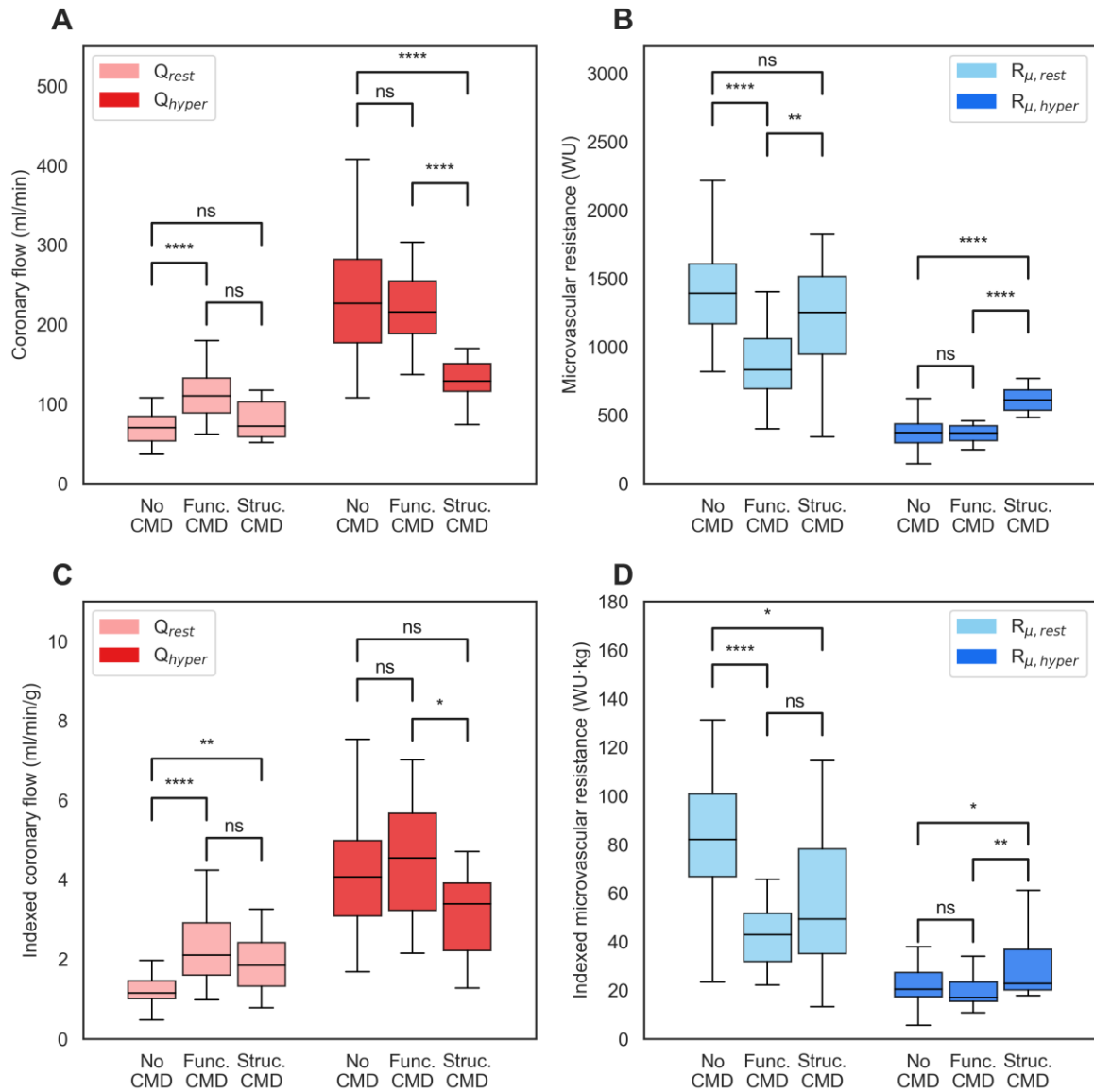
Supplementary Figure 3. Comparison of flow and microvascular resistance parameters in vessels with no CMD (CFR $\geq$2.5; n=54) and those with functional CMD (CFR <2.5 and $R_{\mu,hyp}$ <475 WU; n=32) and structural CMD (CFR <2.5 and $R_{\mu,hyp}$ $\geq$475 WU; n=14): (A) absolute coronary flow (ml/min), (B) absolute microvascular resistance (WU), (C) indexed absolute coronary flow (ml/min/g), (D) indexed absolute microvascular resistance (WU·kg). The displayed symbols correspond to the following p values for pairwise comparisons: ns= $\geq$0.05, * = <0.05, ** = <0.01, *** = <0.001, **** = <0.0001. The Bonferroni correction was applied to p values by multiplying by the number of comparisons performed.
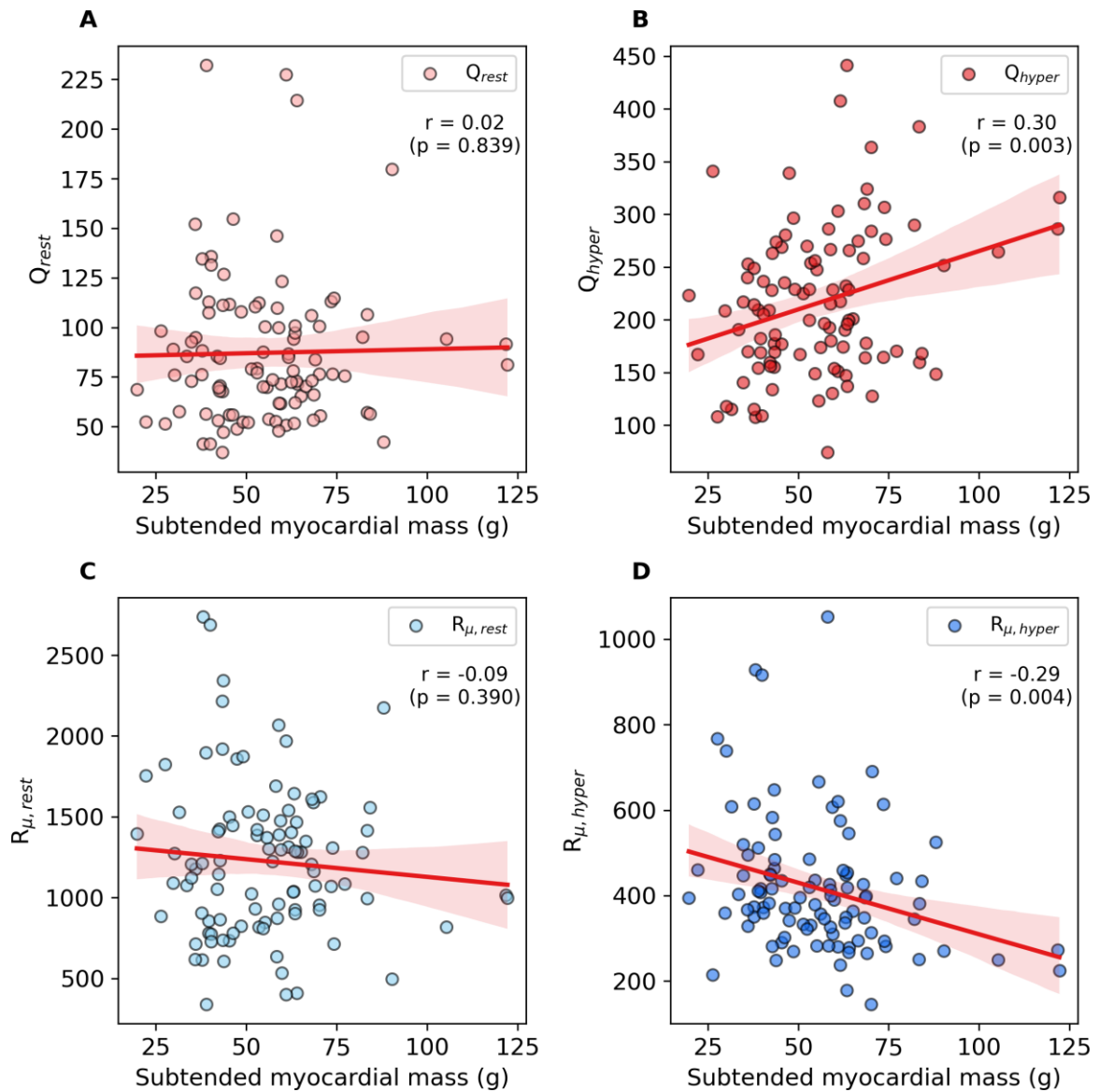
Supplementary Figure 4. Correlation between myocardial mass, absolute coronary flow and microvascular resistance. Correlation between myocardial mass subtended by the left anterior descending artery and: (A+B) absolute coronary flow at rest and during hyperaemia, (C+D) absolute microvascular resistance at rest and during hyperaemia.

Q_{rest} = resting coronary flow; Q_{hyper} = hyperaemic coronary flow; $R_{\mu,rest}$ = resting microvascular resistance; $R_{\mu,hyper}$ = hyperaemic microvascular resistance; WU = Wood units.